

Observation of Collective Atomic Recoil Motion in a Degenerate Fermion Gas

Pengjun Wang (王鹏军),¹ L. Deng,^{2,3} E. W. Hagley,² Zhengkun Fu (付正坤),¹
Shijie Chai (柴世杰),¹ and Jing Zhang (张靖)^{1,*}

¹*The State Key Laboratory of Quantum Optics and Quantum Optics Devices, Institute of Opto-Electronics, Shanxi University, Taiyuan 030006, People's Republic of China*

²*Physical Measurements Laboratory, National Institute of Standards and Technology, Gaithersburg, Maryland USA 20899*

³*Center for Cold Atom Physics and Wuhan Institute of Physics and Mathematics, Chinese Academy of Sciences, Wuhan 430071, China*
(Received 17 June 2010; revised manuscript received 10 December 2010; published 23 May 2011)

We demonstrate collective atomic recoil motion with a dilute, ultracold, degenerate fermion gas in a single spin state. By utilizing an adiabatically decompressed magnetic trap with an aspect ratio different from that of the initial trap, a momentum-squeezed fermion cloud is achieved. With a single pump pulse of the proper polarization, we observe, for the first time, multiple wave-mixing processes that result in distinct collective atomic recoil motion modes in a degenerate fermion cloud. Contrary to the case with Bose condensates, no pump-laser detuning asymmetry is present.

DOI: [10.1103/PhysRevLett.106.210401](https://doi.org/10.1103/PhysRevLett.106.210401)

PACS numbers: 05.30.-d, 03.75.Ss, 67.85.-d

Collective atomic recoil motion involving an internally generated electromagnetic field, also known as matter-wave superradiance [1], is an intriguing process in which a group of atoms in the same electronic state recoils coherently under the excitation of a single laser pulse. Such collective center-of-mass recoil motion modes were first observed by illuminating an elongated Bose-Einstein condensate with a red-detuned, long duration laser pulse of the proper polarization. The resulting atomic scattering pattern was distinctive and highly regular [1]. Since that seminal study it has been argued [1] that the underlying physics of this intriguing process is the scattering of pump photons by a spontaneously generated, matter-wave grating that grows due to positive feedback in the presence of the pump laser [2]. Recently, however, an analytic, small-signal theory [3] has shown that the propagation growth of the scattered field can significantly impact the superradiance process. In a subsequent experimental study [4] with condensates, an efficient suppression of matter-wave superradiance was reported when a blue-detuned pump laser was used. To explain the unexpected pump-laser detuning asymmetry it was postulated [4,5] that the genesis of matter-wave superradiance is fundamentally a multi-matter-optical wave-mixing and propagation process. It was shown that with condensates the ultraslow group velocity of the generated field [3] leads to the coherent buildup of an optical-dipole potential [4,5] that modifies the condensate's structure factor [6], impacts the scattering rate at early times, and results in the pump-laser detuning sign asymmetry.

To date, collective atomic recoil motion by superradiant scattering has only been demonstrated with bosons. The question of whether or not it would be observable with fermions naturally arose, and several theoretical studies based on the matter-wave grating picture have already addressed this issue [7–9]. Experimentally, Yoshikawa,

Torii, and Kuga [10] showed that collective scattering occurs in a thermal, nondegenerate Bose gas. However, the spatial indistinguishability of components scattered from the thermal bosonic cloud with a large momentum spread required the use of spin-flip Raman scattering for state-sensitive probing. While this experiment implies that quantum statistics are not important, matter-wave superradiance has not been directly shown to occur with fermions which obey Fermi-Dirac statistics where atoms cannot occupy the same state because of the Pauli exclusion principle. Furthermore, while it has been shown that the multi-matter-optical wave-mixing process leads to matter-wave superradiance in Bose condensates, to date there has been no experimental evidence of superradiant wave-propagation effects in fermionic systems.

In this Letter we report the first experimental evidence of collective atomic recoil motion in a momentum-squeezed, degenerate fermion gas where the mechanism of bosonic stimulation is obviously absent. We present clear evidence of multiple wave-mixing and propagation processes that lead to multiple collective atomic recoil motion modes. This supports the notion that matter-wave superradiance arises naturally when the atomic center-of-mass motion is included in a nonlinear optical wave-mixing process [3–5]. We further demonstrate that, as predicted in Ref. [4], the red-blue pump-laser detuning asymmetry observed with a Bose condensate is not present. To the best of our knowledge this is the first collective atomic recoil motion and wave-propagation experiment using a momentum-squeezed, degenerate fermion gas. We note that matter-wave superradiance has been considered for highly sensitive matter-wave interferometers, matter-wave amplifiers, and quantum information processors based on ultracold atoms. It is therefore important to better understand this intriguing process and its manifestations in different quantum gases.

We first prepare a degenerate fermion gas in a single spin state by cooling a mixture of $^{87}\text{Rb} + ^{40}\text{K}$ atoms using well-developed evaporative and sympathetic cooling techniques in a quadrupole-Ioffe configuration trap [11] with trapping frequencies $\omega_x/2\pi = 372$ Hz, $\omega_y/2\pi = 186$ Hz, and $\omega_z/2\pi = 24$ Hz. At the end of the cooling process the ^{40}K atomic cloud in the $4S_{1/2}$, $|F = 9/2, m_F = 9/2\rangle$, hyperfine Zeeman state reaches Fermi degeneracy at $T \sim 400$ nK ($\sim 0.3T_F$) with $\sim 2 \times 10^6$ ^{40}K atoms in a fitted size (variance of a Gaussian fit) of $\Delta x \simeq 4.2$ μm , $\Delta y \simeq 8.3$ μm , and $\Delta z \simeq 64.9$ μm [12,13]. All ^{87}Rb atoms are then selectively removed without losing any ^{40}K atoms. The magnetic trap is then decompressed adiabatically to a different aspect ratio, and this results in a momentum-squeezed fermion cloud because there is no thermalization mechanism for the pure sample of ^{40}K atoms. Next, we apply a linearly polarized (along \hat{x}) laser pulse along the \hat{y} direction [Fig. 1(a)]. The magnetic trap is then turned off and linearly polarized probe light propagating along the \hat{x} axis is used to detect the cloud's momentum distribution after a time-of-flight (TOF) sufficient to allow spatial separation of the different momentum components.

Experimentally, we first analyze the momentum distribution of the pure ^{40}K cloud before adiabatic expansion by

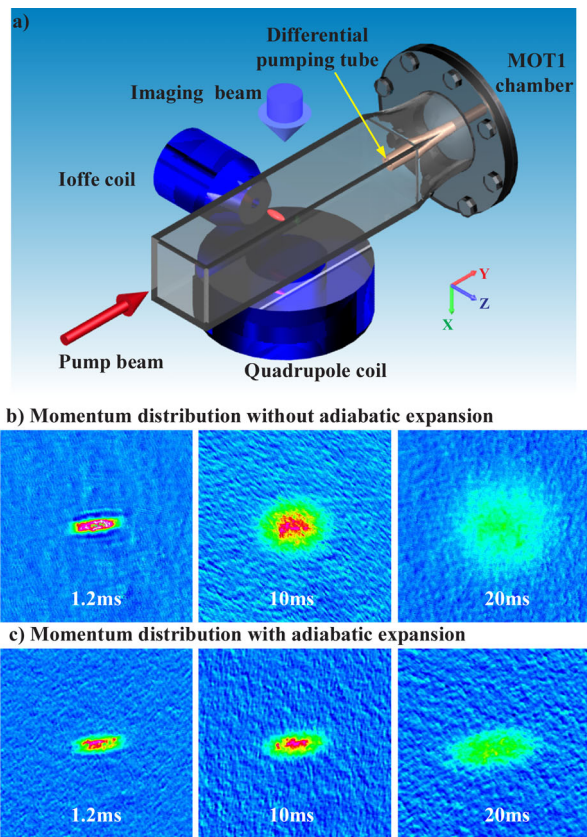


FIG. 1 (color online). (a) Schematic drawing of the experimental setup. (b) Free expansion of a fermion cloud before a controlled adiabatic expansion. (c) Free expansion after a controlled adiabatic expansion. The image size is 1.17 mm by 1.17 mm, and the free expansion times are shown.

turning off the magnetic trap and imaging the freely expanding cloud at different TOFs [see Fig. 1(b)]. After a 20 ms TOF, the size of the fermion cloud (variance of a Gaussian fit) becomes symmetric in the y and z directions with a spatial extent of about $\Delta y \simeq \Delta z \simeq 195$ μm . This corresponds to a momentum spread of $\delta p_y \sim \delta p_z \simeq 1.9\hbar k_L$ (where $k_L = 2\pi/\lambda_L$ and $\lambda_L = 766.7$ nm), and an intrinsic coherence time of $\tau_{y,z} \simeq 40$ μs (calculated using twice the variance). Because the initial momentum spread is above $\hbar k_L$, it would be difficult to unambiguously resolve the collective atomic recoil motion modes. In addition, Pauli blocking may also affect the scattering efficiency because of potential overlap of the initial and final momentum states.

In order to reduce the momentum spread and the effect of Pauli blocking, we subject the atomic cloud to a controlled adiabatic expansion. This critically important step creates a momentum-squeezed, anisotropic degenerate fermion gas that permits unambiguous identification of collective atomic recoil motion modes. Specifically, after the removal of all ^{87}Rb atoms, we adiabatically relax the magnetic trap for 3 seconds such that at the end of the process the trapping frequencies are $\omega_x/2\pi = 66$ Hz, $\omega_y/2\pi = 33$ Hz, and $\omega_z/2\pi = 17$ Hz. After being released from the adiabatically expanded trap it is observed that the momentum spread of the gas mirrors the spatial distribution of the cloud. The result is an elongated, ultracold, momentum-squeezed, degenerate fermion cloud [14] that expands slowly with a nearly fixed aspect ratio [Fig. 1(c)]. A Gaussian fit of the absorption image after a 20 ms TOF reveals a very cold fermion cloud with $\Delta y \simeq 68$ μm . Now the momentum spread of the gas in the primary scattering y direction is $\delta p_y \simeq 0.65\hbar k_L$, permitting clear identification of the scattered and nonscattered fractions because these components will have negligible overlap in momentum and position space after the TOF (note that low-momentum-transfer scatterings may still be impacted by Pauli blocking). The corresponding intrinsic coherence times are $\tau_y \simeq 247$ μs , and $\tau_z \simeq 42$ μs . In the y direction the grating coherence time is $\simeq 9.2$ μs .

Physically, coherent light scattering results in an internally generated electromagnetic field that contributes to the collective atomic recoil motion. Thus, the generation and propagation of this new light field play an important role in matter-wave superradiance. When the familiar description of nonlinear optical wave-mixing and propagation processes [15] are generalized to include atomic recoil motion, matter-wave superradiance arises naturally. Inside the medium excited by the pump laser, photons are first scattered by the usual spontaneous Rayleigh scattering process [15]. These photons are the seed fields that grow coherently in the presence of the pump laser. In the case of a Bose condensate, coherent field growth along the long axis dominates because of the condensate's intrinsically high density and long coherence time. However, for a momentum-squeezed, degenerate fermion gas in a shallow trap, coherent-wave

generation can occur in more general directions, but with significantly smaller gain than with condensates because of the intrinsically lower atomic density and shorter coherence times. For such a low-density medium the competition between coherence time and optical density along the wave-propagation direction is critically important to the coherent buildup of the generated field.

Figure 2(b) is a TOF image of the momentum distribution of the degenerate fermion gas after interacting with a pump-laser pulse. Three distinctive collective atomic recoil motion modes can be clearly identified [see inset in Fig. 2(b)] that bear a strong resemblance to the familiar forward-scattered ($+y$ direction, $2\hbar k_L$ momenta) and $\pm 45^\circ$ ($y \pm z$ directions, $\pm\sqrt{2}\hbar k_L$ momenta) components that one observes with Bose condensates. In the case of condensates, these scattering components are the result of coherent field *propagation* growth along the $\mp z$ directions, and subsequent sequential matter-wave mixing of these first-order components that generates the $2\hbar k_L$ component [1]. However, when coherent propagation growth is important in the degenerate fermion cloud, the scattering efficiency in any direction in the y - z plane is determined by a competition between the effective density, the propagation distance, and the coherence time along the direction of the scattered field. (For atoms scattered out of the original fermion cloud, Pauli blocking is not important.) In our case, we found that the paired components are at $\theta \approx \pm 39^\circ$ with respect to the y axis, instead of the usual $\theta = \pm 45^\circ$. We believe that this occurs because the

coherence time decreases rapidly as the scattering direction swings from the y axis toward the $\pm z$ axis, with the $\pm z$ directions having the shortest coherence time. The competition between the increase in the propagation distance and the decrease of the coherence time results in a locally optimized scattering efficiency at an angle that is smaller than 45° . Indeed, it is clear from Fig. 2(b) that there are more scattered atoms in the regions between the two 39° components than there are in the regions between the z axis and the 39° components. The presence of these modes and the different scattering angle support the matter-optical, wave-mixing, and propagation theory [3].

The explanation of the forward-scattered component is slightly more complicated than that for the $\pm 39^\circ$ components. First, we note that it is unlikely that the forward-scattered component shown in Fig. 2(b) is due to a sequential, second-order process of $\pm 39^\circ$ scattering because such a higher-order scattering must involve a second-order interaction of the weak generated field. More importantly, if such a higher-order process were occurring, there would necessarily be higher-order scattering components in the same $\pm 39^\circ$ directions, as well as a forward component with more than $2\hbar k_L$ of momenta. Lack of these higher-order momentum components indicates that such a second-order process is not present. However, the forward component, which is located at $\approx 390 \mu\text{m}$ from the host cloud (a $2\hbar k_L$ kick corresponds to $396 \mu\text{m}$ for a ^{40}K atom), can be explained by a first-order, wave-mixing process in which an atom absorbs a pump photon traveling in the $+y$ direction and subsequently emits a photon in the $-y$ direction. Experimentally, we took great care to avoid overlapping the fermion gas with any reflection of the pump light from the exit facet of the cell because such a weak reflection could serve as a seed laser for efficient Kapitzi-Dirac scattering [16,17], leading to forward- and backward-scattered components. The fact that no backscattered component was detected in either Fig. 2(b) or the raw images suggests that the Kapitzi-Dirac scattering mechanism was not present. It is thus more probable that the forward component results from a matter-optical-mixing process occurring simultaneously along the y axis [18]. In fact, because this direction has the longest coherence time, we initially expected to observe only this forward-scattered component [see Fig. 1(c) in Ref. [7]].

In Fig. 2(c) we show the integrated optical density distributions of the $0\hbar k_L$, $2\hbar k_L$, and $2\hbar k_L \cos\theta$ components. The Gaussian fits show that the momentum spread of each scattered component is comparable to that of the stationary fermion cloud. This strongly suggests that the collective atomic recoil motion modes have a high degree of coherence, as would be expected from a matter-optical, wave-mixing, and propagation process.

In Fig. 3(a) we show the scattering efficiency of the $\theta = +39^\circ$ component as a function of pulse duration for two different pump powers. The steep rise in the scattered fraction for high pump intensities signals the threshold of

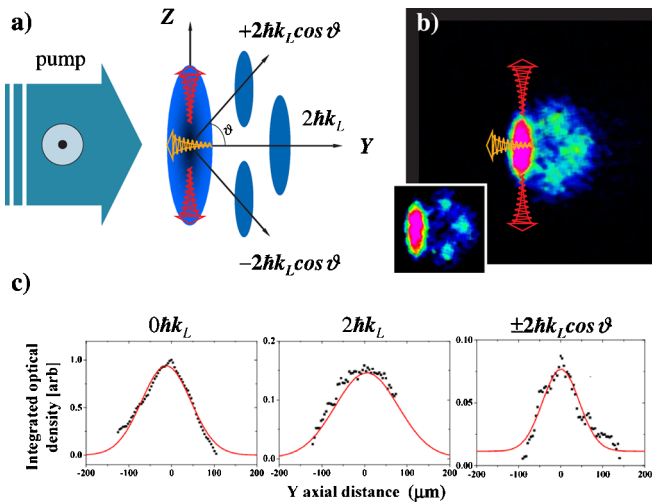


FIG. 2 (color online). Demonstration of collective atomic recoil motion in a momentum-squeezed, degenerate fermion gas. (a) Schematic of experiment. (b) Image (2 mm by 2 mm) of fermion cloud after a 15 ms TOF. The number of atoms in each of the off-axis components is about 10^5 , with slightly more in the forward-scattered component. For this image the laser detuning is $\delta/2\pi = 600$ MHz, the pump-laser Rabi frequency is 13 MHz, and the pump-pulse duration is $100 \mu\text{s}$. The inset's background level was adjusted to clearly identify the location of the scattered peaks. (c) Integrated optical density of each component with a Gaussian fit.

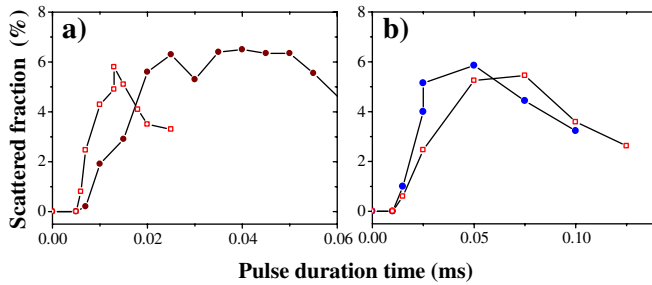


FIG. 3 (color online). Scattering efficiency of $\theta = +39^\circ$ component versus pump-pulse duration. (a) The pump-laser power is 0.15 mW (1.5 mW) for the dots (squares), and the laser detuning is $\delta/2\pi = 300$ MHz for both sets of data which have been rescaled to the same level. (b) For the blue dots (red squares), $\delta/2\pi = +500$ MHz (-500 MHz), and the pump power is 2 mW. The scattering efficiency for the forward component is similar that of the 39° components.

the collective atomic recoil mode. These data are consistent with observations in Bose-condensed gases [1]. For high pump powers the scattering efficiency rises rapidly, but then is followed by a drop of about 40% as the pulse duration increases. A similar drop in efficiency for higher pump powers was also observed with Bose condensates [1], and has already been predicted in numerical studies of superradiance [19].

Finally, we investigated the effect of the sign of the pump-laser detuning on the scattering. A recent experimental study [4] has revealed an efficient suppression of collective atomic recoil motion with Bose condensates pumped by a blue-detuned laser. The key characteristics of Bose condensates that lead to this pump-laser detuning asymmetry are their intrinsically long coherence time and high density, which result in the generation of a growing optical-dipole potential. In the present case, however, because of the much lower density and much shorter coherence times, the gain for the generated field is much smaller and the effect of any induced optical-dipole potential would be negligible. Indeed, Ref. [4] predicted that in a fermion system the scattering efficiency should be independent of the sign of the pump-laser detuning. Figure 3(b) is a plot of the $\theta = +39^\circ$ scattered fraction as a function of pump-laser duration for both red and blue detunings with a fixed pump power. These data, which are consistent with measurements taken at other detunings in the range of $150 \text{ MHz} < |\delta|/2\pi < 600 \text{ MHz}$, clearly show that the red-blue, pump-laser detuning asymmetry observed in Bose condensates is absent. We also note that possible lensing effects due to density inhomogeneity of the fermion gas is small.

In conclusion, we have demonstrated collective atomic recoil motion in a momentum-squeezed, degenerate fermion gas, and have shown that quantum statistics are not critical in the generation of these collective modes. We observed two off-axis collective recoil modes, and demonstrated the importance of field propagation effects.

In contrast to Bose-Einstein condensates, we have shown that the scattering process with fermions is symmetric with respect to the sign of pump-laser detuning. We believe that this work, and our previous studies [3–5], show that matter-wave superradiance arises naturally from nonlinear optical wave-mixing and propagation processes when the atomic center-of-mass motion is included. The occurrence, and even the high growth characteristics, of matter-wave superradiance can be explained in this light. The experiments reported here have opened the possibility of studying matter-wave mixing and amplification with fermions.

Jing Zhang wishes to thank the National Natural Science Foundation of China (Grants No. 10725416, 60821004) and the National Basic Research Program of China (Grant No. 2011CB921601) for financial support.

*Corresponding author.

jzhang74@yahoo.com, jzhang74@sxu.edu.cn

- [1] S. Inouye *et al.*, *Science* **285**, 571 (1999); W. Ketterle and S. Inouye, *C. R. Acad. Sci. IV* **2**, 339 (2001).
- [2] Indeed, Ref. [1] specifically stated that the scattered light does not play any other role in the process other than providing the necessary momentum kick.
- [3] L. Deng, M. G. Payne, and E. W. Hagley, *Phys. Rev. Lett.* **104**, 050402 (2010).
- [4] L. Deng *et al.*, *Phys. Rev. Lett.* **105**, 220404 (2010).
- [5] Xinyu Lou *et al.* (unpublished).
- [6] F. Zambelli *et al.*, *Phys. Rev. A* **61**, 063608 (2000); D. M. Stamper-Kurn *et al.*, *Phys. Rev. Lett.* **83**, 2876 (1999); J. Steinhauer *et al.*, *ibid.* **88**, 120407 (2002).
- [7] W. Ketterle and S. Inouye, *Phys. Rev. Lett.* **86**, 4203 (2001).
- [8] M. G. Moore and P. Meystre, *Phys. Rev. Lett.* **86**, 4199 (2001).
- [9] P. Villain *et al.*, *Phys. Rev. A* **64**, 023606 (2001).
- [10] Y. Yoshikawa, Y. Torii, and T. Kuga, *Phys. Rev. Lett.* **94**, 083602 (2005).
- [11] D. Wei *et al.*, *Chin. Phys. Lett.* **24**, 1541 (2007); D. Xiong *et al.*, *ibid.* **23**, 843 (2008); <http://www.sxu.edu.cn/yjjg/gjzdsys/lab7.htm>.
- [12] For estimating the size of the fermion cloud, see F. Schreck, Ph.D. thesis, ENS, 2002.
- [13] The calculated Fermi radii of the cloud are $R_x = 9.9 \mu\text{m}$, $R_y = 19.9 \mu\text{m}$, and $R_z = 154 \mu\text{m}$. See S. Giorgini, L. P. Pitaevskii, and S. Stringari, *Rev. Mod. Phys.* **80**, 1215 (2008). Throughout this work, we use the variance obtained from a Gaussian fit of the TOF images.
- [14] L. Costa *et al.*, *Phys. Rev. Lett.* **105**, 123201 (2010).
- [15] Y. R. Shen, *The Principles of Nonlinear Optics* (John Wiley & Sons, New York, 1984), 2nd ed.
- [16] G. Gupta *et al.*, *C. R. Acad. Sci. IV-Phys.* **2**, 479 (2001).
- [17] K. Li *et al.*, *Phys. Rev. Lett.* **101**, 250401 (2008).
- [18] Although the images do not indicate any backscattered component, we cannot completely rule out contributions by Kapitzi-Dirac scattering due to a weak diffuse reflection of the pump laser since it is possible that the backscattered component falls below the CCD detection limit.
- [19] O. Zobay and G. M. Nikolopoulos, *Phys. Rev. A* **73**, 013620 (2006).